Baustatik – Baupraxis 14, © 2020, Universität Stuttgart

Advancements in vortex particle methods for aeroelastic analysis of line-like structures

Guido Morgenthal[1], **Igor Kavrakov**[1], **Samir Chawdhury**[1]

[1] *Institute of Structural Engineering, Chair of Modelling and Simulation of Structures, Bauhaus Universität weimar.*

Abstract: The paper presents numerical extensions of Vortex Particle Methods (VPM) for aeroelastic analysis of line-like structures such as long-span bridges. The pseudo-3D VPM is a coupled algorithm that considers the structural behaviour in 3D with flow modelled in 2D. This multi-strip model is able to predict the changes in vorticity flow due to the variation of cross-section along the longitudinal axis. To model inflow fluctuations, the wind field is modelled externally, converted into vortex particles, and finally, they are released in the free stream to introduce turbulence to the downstream section. As an application study, the flutter and buffeting analysis of Great Belt bridge is briefly presented. Another extension is presented for 2D VPM to model large-displacement fluid-structure interaction (FSI) of thin-walled flexible systems. A structural solver based on corotational finite element method is coupled with the 2D VPM to model geometrically nonlinear effects. The flow-induced interaction of T-shape cantilever and flexible membrane roof of a building have been presented.

1 Introduction

Modelling of flows past bluff or moving bodies is very much challenging. Experimental studies are always considered as standard procedures, however the advantages that make the numerical methods increasingly popular are their ability to predict the full-scale aerodynamic behaviour and clear visualization of interesting flow phenomena around bluff or moving flexible bodies. The numerical approaches such as the VPM have gained significant interest in recent years, particularly in the direction of bluff body aerodynamics. The VPM is principally based on the particle discretisation of the vorticity field in a Lagrangian form of the governing Navier-Stokes equations. It has been found to be computationally very efficient for solving 2D FSI problems over the grid-based methods. Initially, the immersed boundary techniques were implemented for the VPM for simulation of flows past bluff bodies of complex geometry [13, 14, 15] for analyses of complex aerodynamic phenomena in long-span bridges. The

technique of seeding vortex particles was implemented further within the mentioned solver to model inflow turbulence for buffeting analyses [3, 2, 8, 9].

2 Advancements in Pseudo-3D Vortex Methods

The high computational cost to conduct a complete 3D CFD analysis inspired advances in the Pseudo-3D approaches that capture the 3D structural behaviour, while modelling the fluid in 2D. The laminar Pseudo-3D Vortex Method attempts to include the structural behaviour in 3D while modelling the fluid in 2D by planes (strips) along the span by employing the strip assumption (cf. Fig. 1, left). It was first used for bridges by Morgenthal and McRobie [12], including further extensions in terms of GPU programming [11] and free-stream turbulence [8]. The structural dynamics can be advanced in both physical or reduced (modal) coordinates (cf. Fig. 1, right). With this, several improvements can be made, despite the simplification of the 3D flow effects. These improvements include: (i) varying cross-sectional geometry along the structure, (ii) varying mean wind speed for each section and most importantly, (iii) the inclusion of an arbitrary number of structural modes which are necessary for adequate representation of 3D structural behaviour.

In case of laminar free-stream, it is reasonable to assume that the self-excited forces are fully correlated over one element, as noted by Scanlan [19]. However, the energy transfer between modes can severely affect the flutter limit and VIV amplitudes, and thus, it is necessary to consider the 3D dynamic behaviour of the structure. For long-span bridges, particular applications of the laminar free-stream Pseudo-3D vortex methods can be the estimation the VIV response and flutter analysis.

The VIV response can be a critical criterion for the serviceability limit state and is typical for deep concrete box girders. As an example, Pseudo-3D analyses were performed on the Niterói bridge by Morgenthal et al. [11]. This bridge is a multi-span double-box concrete girder with a main span of 300 m (cf. Fig. 2, left). The fluid was discretised using 8 strips for two conditions, with and without traffic, and the VIV response was determined. Figure 2 (right) depicts instantaneous velocity field during lock-in. Additionally, the RMS amplitude of the vertical displacements (h_{rms}) at lock-in was validated to the full scale observations presented by Battista and Pfeil [1], yielding good correspondence (cf. Fig. 3, left).

For the ultimate limit state, flutter can be governing. Flutter analysis with high spatial resolution was performed on the Great Belt Bridge by Kavrakov and Morgenthal [7]. With an

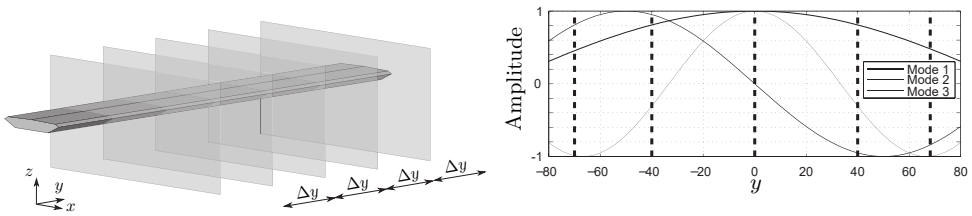

Figure 1: Schematic of the Pseudo-3D method: Multi-strip arrangement along the line-like structure (left) and dynamic representation of the structure through its modes (right).

aerodynamically shaped cross section (cf. Fig. 1, left), the Great Belt Bridge extends with a total span of 2694m, including a main span of 1624m and side spans of 535m. A total of 50 fluid strips and 22 deck modes were used for the Pseudo-3D analysis. The critical flutter speed was determined under laminar free-stream and the results were compared with both experimental results for a taut strip model (cf. Larsen [10]) and semi-analytical results for the linear unsteady aerodynamic model [7]. Figure 3 (right) presents the results, where the semi-analytical results are computed at varying angle of incidence α and then interpolated

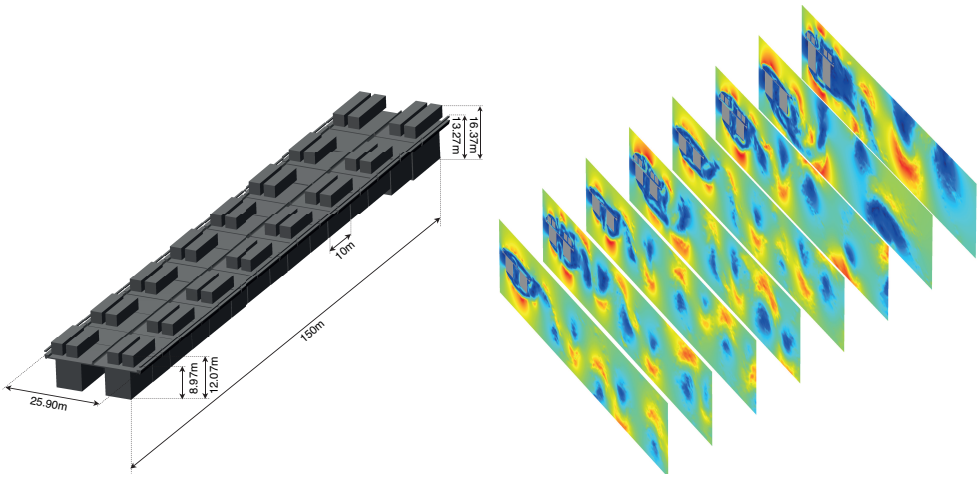

Figure 2: Vortex-induced vibrations of the Niterói bridge: Schematic of the Pseudo-3D model with traffic (one half of main span) (left) and instantaneous velocity fields of the CFD strips (right).

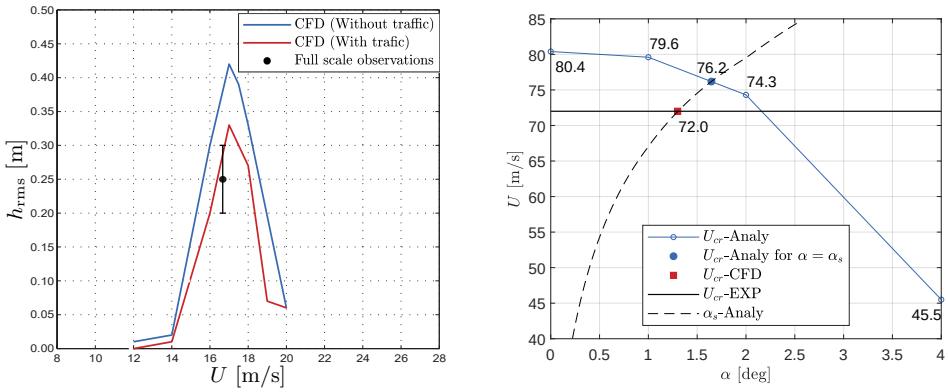

Figure 3: Results from VIV and flutter analyses: Comparison of RMS vertical displacements (h_{rms}) of the VIV analysis of Niterói Bridge for the configurations tested, including full scale observations with confidence interval (cf. Battista and Pfeil [1]) (left). Critical flutter velocity U_{cr} of the Great Belt Bridge including CFD, semi-analytical (at different angle of attack α, including static equilibrium angle α_s), and experimental results (cf. Larsen [10]) (right) .

at the angle of attack for a static equilibrium α_s. This contribution is included automatically for the CFD and experimental results. As it can be seen from the figure, the CFD results correspond well with the experiments. Using the Psuedo-3D Vortex Method, the post-flutter behaviour can be captured as well in terms of LCO. Figure 4 represents two instantaneous particle maps at maximum rotation during LCO, where the contribution of the bending and torsional modes is apparent.

In the case of free-stream turbulence, the 3D effects of the flow are perplexing. In 2D, generating spatially correlated velocities on a sampling ladder upstream of the section and converting them in terms of particles in the fluid domain simulates free-stream turbulence with prescribed statistics (cf. Fig. 5, left). This method is named velocity-based turbulence generation and was developed for 2D by Prendergast [17] and was verified on numerous occasions (cf. e.g. [18, 9]). Kavrakov and Morgenthal [8] combined this method with the laminar Pseudo-3D vortex method, which effectively enabled Pseudo-3D aeroelastic analyses with turbulent free-stream (i.e. buffeting analysis). By means of analytical derivations and numerical experiments, it was shown in [8] that the span-wise coherence between strips of the forces

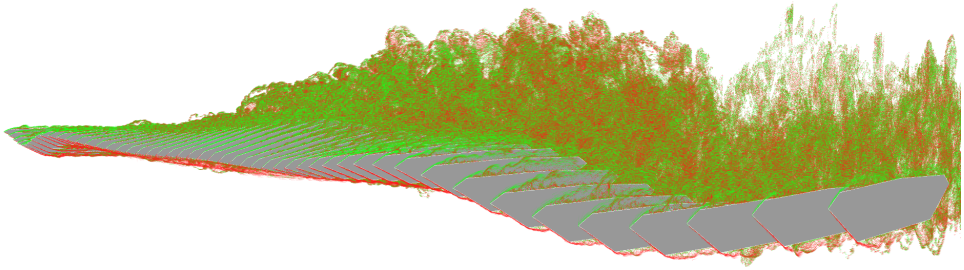

Figure 4: Instantaneous particle maps of the Great Belt Bridge during limit cycle oscillation from Pseudo-3D CFD flutter analysis.

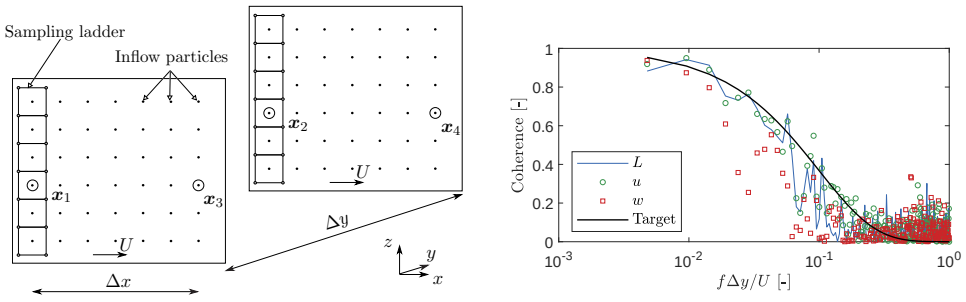

Figure 5: Turbulent Pseudo-3D Vortex Method: Concept for two strips at distance δy including sampling ladders and position of inflow particles convected by the mean velocity U (left). Coherence from a CFD simulation of the lift force L (simulation with bridge deck), longitudinal u and vertical fluctuations w (simulation without bridge deck) between two points ($\boldsymbol{x}_3$ and $\boldsymbol{x}_4$), dependent on the frequency f (right). The target coherence is according to Vickery [20].

and wind fluctuations is retained within the fluid domain (cf. Fig. 5, right). High resolution buffeting analysis using 50 strips was performed on the Great Belt Bridge at a wind speed of U=30 m/s and turbulence intensity of 11% for the longitudinal and 6% for the vertical fluctuations (cf. Fig. 6 for an instantaneous particle map). The results were compared to the results from a semi-analytical analysis using the standard linear unsteady model. The comparison was performed in a statistical manner by using 20 random 10-minute wind records for the semi-analytical analysis, yielding good correspondence (cf. Fig. 7).

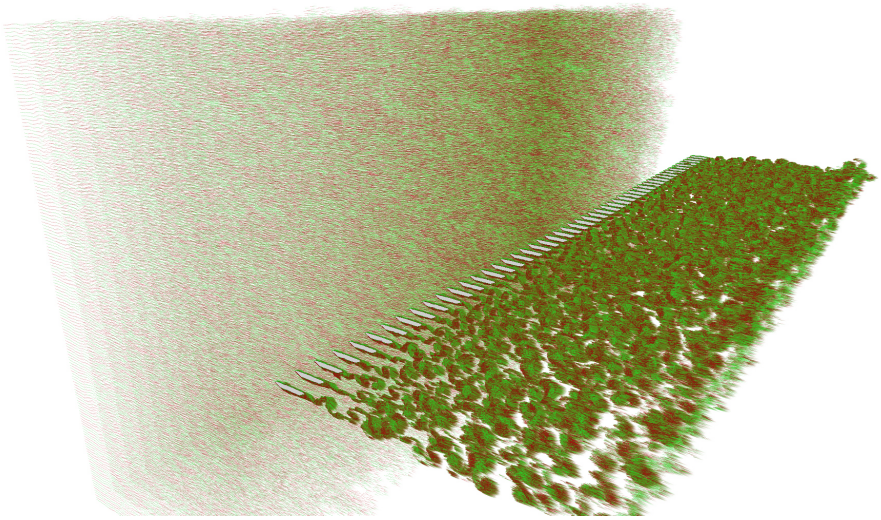

Figure 6: Instantaneous particle map of Great Belt Bridge from Pseudo-3D buffeting analysis.

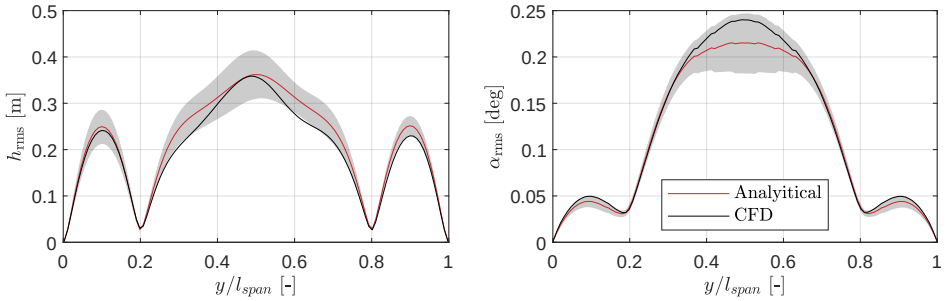

Figure 7: Pseudo-3D buffeting analysis of Great Belt Bridge at a wind speed U =30 m/s: RMS vertical displacements h_{rms} (left) and rotation α_{rms} (right). The results for the CFD model are compared with semi-analytical linear unsteady model. The shaded area defines the 99% confidence interval of the displacements for the analytical model of 20 independent analysis using randomly generated 10-minute wind time-history fluctuations.

3 Fluid-structure interaction of thin-walled systems

FSI problems are frequently encountered in many areas of civil, mechanical, aerospace and biomechanical engineering. The 2D VPM has been coupled with corotational finite element methods (FEM) to perform coupled aeroelastic interactions of thin-walled structures. At each time step the nodal forces are calculated from fluid pressure distribution on the surface panels and supplied to the structural solver. The nodal displacements are projected to surface panels and panel velocities to update the boundary conditions. The details of the method, validation studies, and its several application can be found in [4, 5].

3.1 Aeroelastic fluttering of T-shaped cantilever plates

Aeroelastic instabilities such as the flutter vibration phenomenon are caused by so-called self-excited aerodynamic forces. If aerodynamic forces feed energy into the structure, they act like negative aerodynamic damping which, when it exceeds the mechanical damping, leads to unstable system behaviour. Such vibrations can be used for small-scale energy harvesting [16]. The energy harvesting mechanism from an T-shaped cantilever is presented in Fig. 8. The vibration of the cantilever causes a relative movement between magnets and coils, and thus induces current flow through the circuit. Fig. 9 shows the flow around coupled motion of simulated reference T-shaped cantilever [4]. In wind tunnel, the flutter of the reference T-shaped cantilever initiated at 4 m/s under the mechanical damping only. Fig. 10 shows the numerical identification of flutter for the modelled T-shaped cantilever beam.

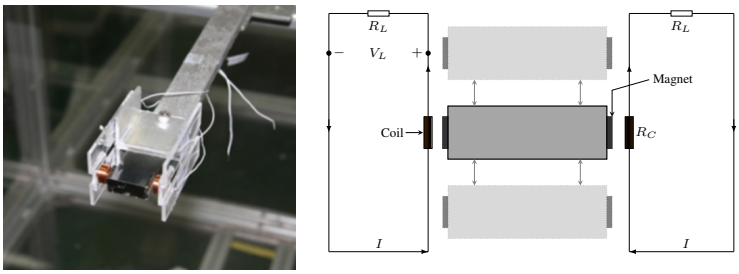

Figure 8: The flutter-induced vibration of T-shaped cantilever for electromagnetic energy harvesting: prototype harvester (left), and circuit diagram (right).

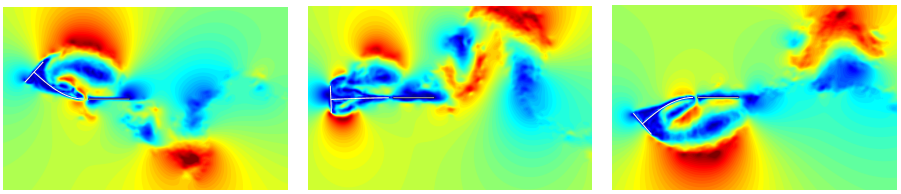

Figure 9: Instantaneous velocity fields around oscillating response T-shaped cantilever system.

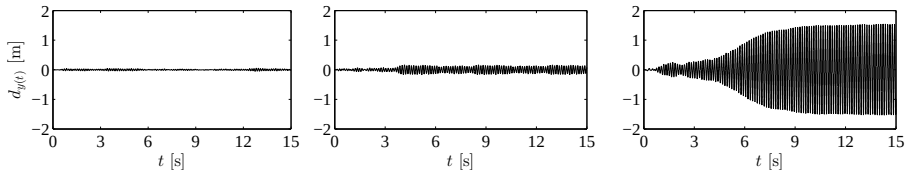

Figure 10: Identification of critical onset flutter wind speed of the reference T-shaped cantilever based on the vertical tip displacement: (left) 2 m/s, (middle) 3 m/s, and (right) 4 m/s.

3.2 Flow over a building with elastic membrane roof

This is a FSI example of an elastic membrane roof system that deals with viscous fluid flow around a building, interacting with nonlinear vibrations of the membrane roof prestressed by gravity loads. It is motivated by a reference FSI case study in which a monolithic coupled approach was modelled using space–time finite elements [6]. A schematic of the modified problem is shown in Fig. 11. The surface boundary layer is modelled by considering thin plates. Here, the free stream flow velocity U_∞ is considered 13.75 m/s.

In order to model the ground surface before and behind the building, two rectangular thin-plates are considered. Overall, 658 panels have been used for this simulation. The flexible roof is discretised into 50 beam elements. According to the reference study, the horizontal and non-prestressed membrane roof is considered to be loaded by 32 % of the dead load. Initially, a static analysis of the membrane roof, building and surrounding surface boundaries is performed to understand the vortex shedding pattern. The total number of particles are found to be in between 110,000 and 130,000. The study results are summarized in Fig. 12. The vortices stay for some times behind the building and increase until the diameter exceeds the building height. The mean plus/minus one standard deviation profiles shows the generation of vorticity behind the building. The dominant frequency of the monitored vertical flow velocity at $x = 25$ m and $y = 5.3$ m is found to be 0.125 Hz.

Now, the flexible membrane roof is considered only for geometrically nonlinear structural dynamics. A more or less periodical system behaviour occurs after 35 s with frequencies of 0.9–1.0 Hz, and the vertical displacements of the membrane at the centre (d_y at point B) are found to be 15–20 cm (see Fig. 13). The response amplitudes and the frequencies are found to be very much similar as they were mentioned in the reference study.

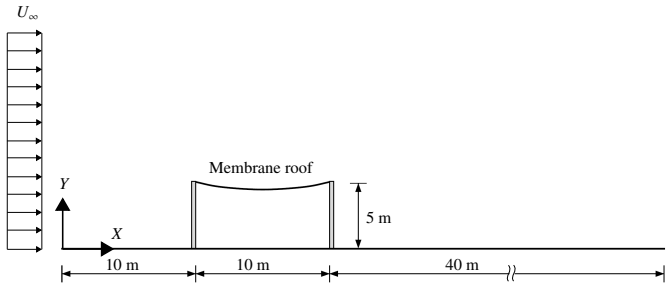

Figure 11: The schematic of uniform flow over a membrane roof of a building.

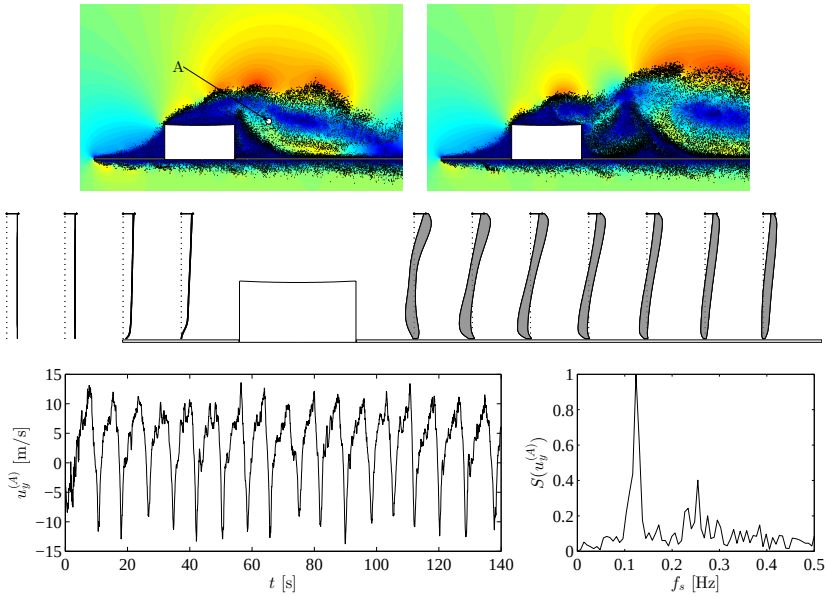

Figure 12: Simulation of flow around the rigid building with flexible roof: Separation of flow at leading edge, whereas the vortex shedding occurs at trailing edge (top). The statistical velocity profiles $(\bar{u_y} \pm \sigma_{u_y})/U_\infty$ at the monitored sections under $U_\infty = 13.75$ m/s (middle). The time history of the vertical flow velocity behind the building (monitored point A) (left) and the frequency spectrum of the velocity signal (right).

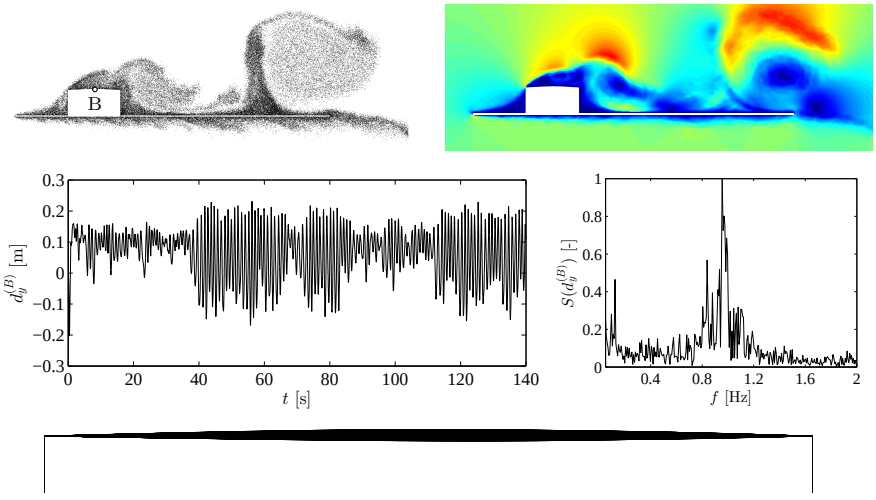

Figure 13: Aeroelastic response of flexible membrane roof at flow velocity 13.75 m/s (displacement is positive upward): The particle map and corresponding flow fields (top). A point "B" is marked at the roof centre where the vertical displacements ($d_y^{(B)}$) are monitored. The displacement time history and corresponding frequency spectrum (middle). The envelope of the dynamic responses of the membrane roof (bottom).

4 Conclusion

The paper has presented several advancements to the vortex methods for aeroelastic response analysis of line-like structures. The laminar and presented turbulent Pseudo-3D VPM provide a new framework to unveil some of the nonlinear and local non-stationary effects for wind-bridge interaction. Utilizing the Pseudo-3D VPM, the vortex shedding, local turbulence effects and aerodynamic nonlinearities are inherent in a 2D manner. Thus, this provides an advantage over the reduced-order (semi-analytical) aerodynamic model, especially for high amplitudes of oscillation and severe wind conditions. It is indented that the method is considered from a modelling aspect, rather than as a simulation, serving as a compromise between the limitations of the semi-analytical models and high computational demand of the 3D CFD simulations. The coupled extension of 2D VPM has shown its ability to simulate large-displacement FSI simulations of thin-walled systems. The nonlinear response of the T-shaped system has been well predicted when compared to the flutter limit in the wind tunnel experiment. The flexible behaviour and coupled dynamic response of roof under the consideration of prestressing due to dead load are also well modelled when compared to a reference study. The method has represented its potential to handle FSI problems in which a partially flexible system can be influenced additionally by the rigid bodies in incoming flow.

References

[1] BATTISTA, R. ; PFEIL, M. : Reduction of vortex-induced oscillations of Rio-Niterói bridge by dynamic control devices. In: *J. Wind Eng. Ind. Aerodyn.* 84 (2000), S. 273–288

[2] CHAWDHURY, S. ; MILANI, D. ; MORGENTHAL, G. : Modeling of pulsating incoming flow using vortex particle methods to investigate the performance of flutter-based energy harvesters. In: *Computers & Structures* 209 (2018), S. 130–149

[3] CHAWDHURY, S. ; MORGENTHAL, G. : Flow reproduction using Vortex Particle Methods for simulating wake buffeting response of bluff structures. In: *Journal of Wind Engineering and Industrial Aerodynamics* 151 (2016), S. 122–136

[4] CHAWDHURY, S. ; MORGENTHAL, G. : Numerical simulations of aeroelastic instabilities to optimize the performance of flutter-based electromagnetic energy harvesters. In: *Journal of Intelligent Material Systems and Structures* 29 (2018), Nr. 4, S. 479–495

[5] CHAWDHURY, S. ; MORGENTHAL, G. : A partitioned solver to simulate large-displacement fluid–structure interaction of thin plate systems for vibration energy harvesting. In: *Computers & Structures* 224 (2019), S. 106110

[6] HÜBNER, B. ; WALHORN, E. ; DINKLER, D. : A monolithic approach to fluid–structure interaction using space–time finite elements. In: *Computer methods in applied mechanics and engineering* 193 (2004), Nr. 23-26, S. 2087–2104

[7] KAVRAKOV, I. ; MORGENTHAL, G. : A Comparative Assessment of Aerodynamic Models for Buffeting and Flutter of Long-Span Bridges. In: *Eng.* 3 (2017), S. 823–838

[8] KAVRAKOV, I. ; MORGENTHAL, G. : Aeroelastic analyses of bridges using a Pseudo-3D vortex method and velocity-based synthetic turbulence generation. In: *Eng. Struct.* 176 (2018), S. 825–839

[9] KAVRAKOV, I. ; MORGENTHAL, G. : A synergistic study of a CFD and semi-analytical models for aeroelastic analysis of bridges in turbulent wind conditions. In: *J. Fluids Struct.* 82 (2018), S. 59–85

[10] LARSEN, A. : Aerodynamic aspects of the final design of the 1624m suspension bridge across the Great Belt. In: *J. Wind Eng. Ind. Aerodyn.* 48 (1993), S. 261–285

[11] MORGENTHAL, G. ; CORRIOLS, A. ; BENDIG, B. : A GPU-accelerated Pseudo-3D vortex method for aerodynamic analysis. In: *J. Wind Eng. Ind. Aerodyn.* 125 (2014), S. 69–80

[12] MORGENTHAL, G. ; MCROBIE, F. : A comparative study of numerical methods for fluid-structure interaction analysis in long-span bridge design. In: *Wind Struct.* 5 (2002), S. 101–114

[13] MORGENTHAL, G. ; WALTHER, J. H.: An immersed interface method for the vortex-in-cell algorithm. In: *Computers & structures* 85 (2007), Nr. 11-14, S. 712–726

[14] MORGENTHAL, G. : Aerodynamic analysis of structures using high-resolution vortex particle methods. In: *PhD thesis, University of Cambridge* (2002)

[15] MORGENTHAL, G. : Advances in numerical bridge aerodynamics and recent applications. In: *Structural engineering international* 15 (2005), Nr. 2, S. 95–95

[16] PARK, J. ; MORGENTHAL, G. ; KIM, K. ; KWON, S.-D. ; LAW, K. H.: Power evaluation of flutter-based electromagnetic energy harvesters using computational fluid dynamics simulations. In: *Journal of Intelligent Material Systems and Structures* 25 (2014), Nr. 14, S. 1800–1812

[17] PRENDERGAST, J. : *Simulation of 2D unsteady wind by a vortex method*, Cambridge University, Diss., 2007

[18] RASMUSSEN, J. T. ; HEJLESEN, M. M. ; LARSEN, A. ; WALTHER, J. H.: Discrete vortex method simulations of the aerodynamic admittance in bridge aerodynamics. In: *J. Wind Eng. Ind. Aerodyn.* 99 (2010), S. 776–785

[19] SCANLAN, R. H.: Amplitude and turbulence effects on bridge flutter derivatives. In: *J. Struct. Eng.* 123 (1997), S. 232–236

[20] VICKERY, B. J.: On the reliability of gust loading factors. In: *Proc. of Tenchincal meeting concerning wind loads on buildings and structures*. Maryland, USA, 1969, S. 93–104